ORIGINAL ARTICLE

Journal of Cachexia, Sarcopenia and Muscle 2021; **12**: 1079–1097
Published online 18 May 2021 in Wiley Online Library (wileyonlinelibrary.com) **DOI:** 10.1002/jcsm.12714

Activated mast cells in skeletal muscle can be a potential mediator for cancer-associated cachexia

D. Brooke Widner[1], Chun Liu[2], Qingxia Zhao[1], Sarah Sharp[1,3], Matthew R. Eber[1], Sun H. Park[1], D. Clark Files[2] & Yusuke Shiozawa[1]*

[1]*Department of Cancer Biology and Comprehensive Cancer Center, Wake Forest University Health Sciences, Winston-Salem, NC, USA;* [2]*Internal Medicine-Sections in Pulmonary and Critical Care Medicine and Geriatrics and the Critical Illness Injury and Recovery Research Center, Wake Forest University Health Sciences, Winston-Salem, NC, USA;* [3]*Department of Biology, Wake Forest University, Winston-Salem, NC, USA*

Abstract

Background Eighty per cent of United States advanced cancer patients faces a worsened prognosis due to cancer-associated cachexia. Inflammation is one driver of muscle atrophy in cachexia, and skeletal muscle-resident immune cells could be a source of inflammation. This study explores the efficacy of cancer activated skeletal muscle-resident mast cells as a biomarker and mediator of cachexia.

Methods Individual gene markers for immune cells were assessed in a publicly available colon carcinoma cohort of normal ($n = 3$), moderate cachexia ($n = 3$), and severe cachexia ($n = 4$) mice. Lewis lung carcinoma (LL/2) cells induced cachexia in C57BL/6 mice, and a combination of toluidine blue staining, immunofluorescence, quantitative polymerase chain reaction, and western blots measured innate immune cell expression in hind limb muscles. *In vitro* measurements included C2C12 myotube diameter before and after treatment with media from primary murine mast cells activated with LL/2 conditioned media. To assess translational potential in human samples, innate immune cell signatures were assessed for correlation with skeletal muscle atrophy and apoptosis, dietary excess, and cachexia signatures in normal skeletal muscle tissue. Gene set enrichment analysis was performed with innate immune cell signatures in publicly available cohorts for upper gastrointestinal (GI) cancer and pancreatic ductal adenocarcinoma (PDAC) patients (accession: GSE34111 and GSE130563, respectively).

Results Individual innate immunity genes (TPSAB1 and CD68) showed significant increases in severe cachexia (weight loss $> 15\%$) mice in a C26 cohort (GSE24112). Induction of cachexia in C57BL/6 mice with LL/2 subcutaneous injection significantly increased the number of activated skeletal muscle-resident degranulating mast cells. Murine mast cells activated with LL/2 conditioned media decreased C2C12 myotube diameter ($P \leq 0.05$). Normal human skeletal muscle showed significant positive correlations between innate immune cell signatures and muscle apoptosis and atrophy, dietary excess, and cachexia signatures. The mast cell signature was up-regulated (positive normalized enrichment score and false discovery rate ≤ 0.1) in upper GI cachectic patients ($n = 12$) compared with control ($n = 6$), as well as in cachectic PDAC patients ($n = 17$) compared with control patients ($n = 16$).

Conclusions Activated skeletal muscle-resident mast cells are enriched in cachectic muscles, suggesting skeletal-muscle resident mast cells may serve as a biomarker and mediator for cachexia development to improve patient diagnosis and prognosis.

Keywords Cancer-associated cachexia; Mast cells; Degranulation; Innate immunity; Skeletal muscle

Received: 15 September 2020; Revised: 14 April 2021; Accepted: 19 April 2021
**Correspondence to: Yusuke Shiozawa, Wake Forest University Health Sciences, Medical Center Blvd, Winston-Salem, NC 27157-1082, USA. Phone: 336-716-8743, Fax: 336-716-0255, Email: yshiozaw@wakehealth.edu*

Introduction

In general, 50% of all collective cancer patients, and 80% of all advanced cancer patients, in the United States will experience rapid weight loss of 5% or more of their total body weight within a 6 month timeframe. This condition is clinically designated as cancer-associated cachexia[1,2] and is concomitant with both a reduced quality of life and an overall worsened prognosis.[1,3] Indeed, one-third of all cancer-related deaths are now being attributed to cancer-associated cachexia, due to cachexia-driven systemic organ failure.[1,4] Historically, the strategy for caring for cachexia patients has been to focus on treating the cancer. Unfortunately, cancer treatments are inherently more difficult in cachectic patients who are often unable to undergo major surgeries and full chemotherapy treatments.[3,4] Patients in the final stage of cachexia, no longer respond to any form of cancer treatment, and weight loss continues to progress in spite of increased nutrient intake or supplementation.[2] As a result, treatment plans for these patients are primarily palliative in nature.[2,5] To date, there are no standard approved therapeutic options for cancer-associated cachexia.

Cancer-associated cachexia is an incredibly complex and variable metabolic syndrome, making both treatment and early identification of at-risk patients a challenge.[6,7] A general consensus in the field is that the condition's characteristic skeletal muscle mass loss is due to a combination of increased protein degradation and decreased protein synthesis. This imbalance between degradation and synthesis is thought to largely be driven by inflammatory factors, such as tumour-necrosis factor-α and interleukin 6 (IL-6).[1,3,5,6,8–10] However, the usefulness of these circulating cytokines as biomarkers for the development of cachexia has been met with variable levels of success.[5,6] Additionally, while specific inflammatory cytokine inhibitors have been tested in therapeutic studies for cancer-associated cachexia, these studies have been largely ineffective in part due to targeting only individual cytokines.[6,11,12] One strategy for overcoming this obstacle to treatment, is to examine common sources of these inflammatory cytokines, such as cells from the adaptive or innate immune system. One potential cell type fitting this description is the mast cells.[13]

Mast cells are granulocytes most commonly known for their role in allergies. They circulate throughout the body in their progenitor form, and then upon differentiation move to reside in tissues as a long-lived sentinel cell of the innate immune system. Upon activation through a stimulus, mast cells will degranulate and release inflammatory mediators, including histamine, cytokines, and proteases into the surrounding area, rapidly triggering an inflammatory response and attracting additional immune cells to the area.[13,14] Following this initial release of inflammatory factors, mast cells will then proceed to generate additional inflammatory mediators through *de novo* synthesis, increasing inflammation over time. Furthermore, differentiated mature mast cells reside naturally in the connective tissue, between individual skeletal muscle fibres, making them an immediate source of inflammation in muscle tissue. Notably, mast cells have been previously implicated in the inflammatory myopathy, polymyositis,[15] as well as in the genetic disorder Duchenne muscular dystrophy,[16] but have not been looked at in depth for their role in cancer-associated cachexia. Examining the presence and activation of resident skeletal muscle mast cells in cachectic samples is necessary to ascertain the usability of mast cells as a biomarker for cachexia development, as well as present a potential new therapeutic target for the treatment or prevention of cancer-associated cachexia.

In this paper, a combination of *in vivo*, *in vitro*, and bioinformatics techniques were used to assess the presence of immune cells in cachectic muscle tissue. A mouse colon carcinoma cachexia cohort showed changes in genes associated with innate immune cell genes, but not adaptive immune cell genes.[17–19] The Lewis lung carcinoma (LL/2) model showed an increase in degranulating skeletal muscle-resident mast cells in cachectic mice compared with their non-cancer controls, while there was no significant change in the number of macrophages and neutrophils. Subsequently, murine mast cells were activated to degranulate through secreted factors from the LL/2 cells, and the activated mast cells decreased fibre size of murine C2C12 myotube cultures. Finally, human cohorts showed increased expression of mast cell activation signature in cachectic patients, as well as correlations with muscle apoptosis and atrophy signatures with the mast cell signature in normal muscle tissues.[18–30]

Materials and methods

Cell culture

The murine mastocytoma P815, lung carcinoma LL/2, and myoblast C2C12 cell lines were purchased from the American Type Culture Collection (ATCC, Manassas, VA). Cells lines were cultured in Dulbecco's Modified Eagle's Medium (DMEM) (Gibco, Waltham, MA), supplemented with 10% (*V*/V) foetal bovine serum (Gibco), 1% (V/V) penicillin and streptomycin (Gibco), and 1% (V/V) L-glutamine (Gibco), and all plates were maintained at 37°C with 5% CO_2.

Cachectic mouse model

Male C57BL/6 J mice (Jax Stock #00064) were purchased from Jackson Laboratories (Bar Harbour, ME). Mice were housed with ad libitum access to food and water. All experiments abided by the Institutional Animal Care and Use Committee (IACUC) guidelines of Wake Forest University Health Sciences

(Protocol A18-026). Male 5-month-old mice were inoculated with either 2.0×10^6 LL/2 cells in 100 μL of DMEM or 100 μL of serum-free DMEM through subcutaneous injection into the right flank. Tumour volume was tracked using a calliper, starting 10 days after injection of the tumour cells. Daily body mass was recorded for each mouse. The average daily food intake per mouse was calculated based on the average food consumed per each cage of five mice. At the time of harvest, tumour mass and tumour-free body mass were measured, following excision of the tumour.

Force transducer assays for muscle function

An *in vivo* force transducer (Aurora Scientific, Aurora, ON, Canada) was used for force frequency and time to fatigue measurements.[31] Electrodes stimulated plantarflexion of the right hind limb. The maximum contractile force [the highest elicited force following excitation with a range of increasing electrical stimulation frequencies (e.g. 20, 40, 60, 80, 100, 125, 150, 200, 250, and 300 Hz) every 2 min with a force transducer] was recorded. Time to muscle fatigue (the time it takes for the maximum force generated to decrease by 50% in response to repeated electrode stimulation at 60 Hz) was also recorded, following 5 min of rest.

Excised muscle measurements and immunostaining

The excised muscle mass of the soleus (SOL), extensor digitorum longus (EDL), tibialis anterior (TA), and gastrocnemius (GA) muscles were measured at harvest. Muscles were snap-frozen in liquid nitrogen for cryosectioning and immunostaining. Transverse sections were made using a Leica CM3050 S cryostat (Leica Biosystems, Wetzlar, Germany) to prepare 20 μm of thick sections on slides for immunofluorescence or immunohistochemistry staining. All microscopy quantifications were performed using three sections per muscle per mouse.

Muscle wasting was assessed using a wheat germ agglutinin Alexa Fluor 488 conjugate (Invitrogen, Waltham, MA, cat #: W11261) to measure muscle fibre cross-sectional area of the transverse sections. Images were taken at 10× magnification to cover 80–100% of muscle tissue (one image per section for EDL and SOL tissues, three images per section for GA and TA tissues). Cross-sectional area quantification was performed using ImageJ (National Institutes of Health, Bethesda, MD).

In some cases, muscle sections were stained with toluidine blue (Sigma-Aldrich, St. Louis, MO, cat #: T3620), CD68 (Abcam, Cambridge, MA, cat #: 125212), and neutrophil elastase (NE) (Abcam, cat #: 68672) primary antibodies, and Cy-3 conjugated-AffiniPure Donkey Anti Rabbit IgG secondary antibody (Jackson ImmunoResearch Laboratories, West Grove, PA, cat #: 711-165-152), according to the manufacturer's instructions. The number of total and degranulating mast cells encompassed in the skeletal muscle endomysium and perimysium were quantified using 40× images. Images were coded and randomized to allow for blinded quantification without knowledge of the cachexia status of the mice. Muscle sections stained for CD68 and NE underwent citrate buffer antigen retrieval, as previously described.[32] The total number of CD68 and NE positive staining were quantified using 20× images and ImageJ to set a minimum staining intensity threshold for positive staining.

Quantitative polymerase chain reaction of muscle ubiquitin ligases and immune cell genes

Excised muscles were homogenized with a pestle and lysed using a Direct-Zol Mini Prep lysis kit (Zymo Research, Irvine, CA) according to the manufacturer's instructions. The GA and TA tissues from each mouse were lysed individually. The EDL and SOL tissues were pooled within groups and lysed. cDNA was prepared from the lysed samples, and quantitative polymerase chain reaction was run using tripartite motif containing 63 (TRIM63) (Mm01185221_m1), F-box protein 32 (FBXO32) (Mm00499523_m1), tryptase alpha/beta 1 (TPSAB1) (Mm00491950_m1), tryptase beta 2 (TPSB2) (Mm00487645_m1), CD68 (Mm03047343_m1), and neutrophil elastase gene (ELANE) (Mm00469310_m1) target primers, with GAPDH (Mm99999915_g1) as a housekeeping gene (TaqMan Applied Biosystems, Waltham, MA). Relative gene expression was calculated using the $2^{-\Delta\Delta CT}$ values.

Western blots

Excised muscles were homogenized with a pestle and lysed for protein in RIPA Lysis and Extraction buffer (Fisher Scientific) with EDTA-free protease inhibitor cocktail (Sigma-Aldrich). All muscles were lysed individually. Likewise, differentiated C2C12 myotubes were lysed following a 24 h incubation with the indicated conditioned media. Western blots were run using antibodies for tryptase (Abcam, cat #: ab151757), Mas-related gene X2 (MrgX2) (1:1000, Novus Biological, Littleton, CO, cat #: NB110-75035), CD68 (1:1,000, Abcam, cat #: ab125212), myeloperoxidase (MPO) (1:1000, Abcam, cat #: ab208670), muscle-specific RING finger-1 (MuRF1) (1:1000, Santa Cruz Biotechnology, Dallas, TX, cat #: sc-398608), muscle atrophy F-box (MAFbx) (1:1000, Santa Cruz Biotechnology, cat #: sc-166806), and fast myosin skeletal heavy chain (MyHC) (1:1,000, Abcam, cat #: ab91506). GAPDH (1:5000, Cell Signalling Technology, Danvers, MA, cat #: 2118) was used as the loading control.

Expression of target proteins was normalized based on GAPDH expression using ImageJ.

LL/2 conditioned media collection

LL/2 cells were plated in 10 cm dishes at a concentration of 10×10^5 cells/mL in serum-free DMEM for 24 h. Conditioned media (CM) was concentrated using a 10 kDa cut-off Ultra Centrifugal Filter Unit (Millipore Sigma, Burlington, MA).

Measuring lysosome-associated membrane protein 2 (LAMP2) expression with flow cytometry

Lysosome-associated membrane protein 2 (LAMP2) expression was measured, as previously described.[33] Briefly, P815 cells were washed and resuspended in HEPES Buffer with 5% (V/V) bovine serum albumin. Cells were treated with either HEPES buffer, concentrated LL/2 CM, or concentrated DMEM (control CM) for 10 min. The reaction was stopped, cells were labelled with LAMP2 antibody (BioLegend, San Diego, CA, cat #: 108505), and analysed by flow cytometry with a BD Accuri C6 Analyser flow cytometer (BD Biosciences, San Jose, CA). Assay was repeated three times.

Primary bone marrow-derived mast cells culture

Primary bone marrow-derived mast cells (BMMCs) were established *in vitro*, as previously described.[34] Briefly, excised femurs and tibias from 6-week-old male C57BL/6 mice were flushed with Roswell Park Memorial Institute 1640 media (Gibco) supplemented with 10% (V/V) foetal bovine serum (Gibco), 1% (V/V) penicillin and streptomycin (Gibco), 1% (V/V) L-glutamine (Gibco), 1% HEPES buffer (Fisher Scientific, Waltham, MA), and 50 μM 2-mercaptoethanol (Fisher Scientific). Resulting cells were cultured in complete mast cell media containing recombinant murine IL-3 (PeproTech Cranbury, NJ, cat #: 213-13) to promote mast cell maturation for 4 weeks and were used within 6 weeks. The purity of the mature population was confirmed using a BD Accuri C6 Analyser flow cytometer (BD Biosciences) following a 30 min incubation with antibodies for both c-Kit-allophycocyanin (APC) (Biolegend, cat #: 105812) and IgER-fluorescein isothiocyanate (eBioscience, San Diego, CA, cat #: 11-5898-82). Mast cells are double positive for c-Kit and IgER.[34]

Interleukin 6 release of activated mast cells

Bone marrow-derived mast cells were cytokine starved overnight without IL-3 prior to plating. BMMCs were plated in a 24 well plate at a concentration of 5×10^5 cells/mL. Cells were treated with either concentrated LL/2 or control CM for 24 h. The concentration of IL-6 in the CM was measured in triplicate using an ELISA kit (R&D Systems, Minneapolis, MN) according to the manufacturer's protocol.

C2C12 myotube diameter measurement

Changes in differentiated C2C12 myotube diameter in the presence of conditioned media or fresh growth media was measured using basic microscopy and quantitative software (ImageJ), as previously described.[35] Briefly, 90% confluent C2C12 cells were incubated with media containing 2% (V/V) horse serum (Gibco) to promote formation of myotubes. Media was changed every 48 h for 7 days. After 7 days of incubation, the myotubes were treated with 10 μM cytosine arabinoside hydrochloride (Sigma-Aldrich, cat #: C6645) for 3 days to remove remaining myoblasts.[35] Myotubes were treated with fresh growth media (Control CM), LL/2 CM, BMMC CM, or LL/2-pre-activated BMMC CM. Myotube cultures were photographed prior to treatment and 24 h following treatment. Average myotube diameter for each well was calculated using five random fields of view at 40× magnification captured with an EVOS XL Core Cell Imaging System (Invitrogen). For each field the diameter of five myotubes was calculated using 10 random points along the myotube. Images were coded to allow for blinded quantification without knowledge of the treatment conditions of the wells. Data were normalized according to average myotube diameter of the control wells.

Bioinformatics

The Gene Expression Omnibus was used to access genomics data available for murine C26 cachexia model (GSE24112), and human upper gastrointestinal (GI) cancer (GSE34111) or pancreatic ductal adenocarcinoma (GSE130563) cohorts.[17–21,30] Molecular signatures for immune cell activation were obtained from the Molecular Signatures Database (MSigDB, accessed in 2019) and were contributed by the Gene Ontology Consortium.[22–26] Molecular signatures for dietary excess (reflecting heightened energy expenditure) and cachexia were also obtained from MSigDB (accessed in 2021) and were contributed by the Gene Ontology Consortium and The Jackson Laboratory Human Phenotype Ontology Group, respectively.[36]

Signatures used are listed below:

GO_MAST_CELL_MEDIATED_IMMUNITY
GO_NEUTROPHIL_ACTIVATION_INVOLVED_IN_IMMUNE_RESPONSE
GO_MACROPHAGE_ACTIVATION_INVOLVED_IN_IMMUNE_RESPONSE
GO_POSITIVE_REGULATION_OF_MUSCLE_CELL_APOPTOTIC_PROCESS

GO_MUSCLE_ATROPHY
ADAPTIVE_IMMUNE_RESPONSE (GO:0002250)
INNATE_IMMUNE_RESPONSE (GO:0045087)
GO_RESPONSE_TO_DIETARY_EXCESS (GO:0002021)
HP_CACHEXIA (HP:0004326)

Gene Set Enrichment Analysis (v4.0.3) was used to measure enrichment of these signatures within the human cohorts to examine enrichment in cachectic patients.[24,27] The Gene Expression Profiling Interactive Analysis (GEPIA) was used to access correlation between the innate immune cell signatures and muscle atrophy or apoptosis signatures listed above in normal muscle tissue from the Genotype-Tissue Expression project as linked on the GEPIA2 website.[28,29] Correlation analysis was expressed using the Spearman correlation.

Statistical analyses

Numerical data are expressed as mean ± standard error of the mean (SEM). Statistical analysis was performed using the GraphPad Prism statistical program (GraphPad Software, San Diego, CA) with significance at $P \leq 0.05$. An unpaired Student's *t*-test or one-way analysis of variance (ANOVA) with Tukey's or Bonferroni's post-test was used to compare single measurements between groups where indicated. A two-way ANOVA was used to compare between groups with multiple or repeated measurements.

Results

Increased expression of innate immune cell genes in a cachexia model

To address whether muscle-resident immune cells, including mast cells, are involved in the pathogenesis of cancer-associated cachexia, first the association between the cancer-associated cachexia condition and expression of genes commonly associated with cells from the innate and adaptive immune system was assessed (*Figure* 1A & B). To do so, a publicly available cohort was used, which examined array-based gene expression profiling of quadriceps muscles from CD2F1 mice bearing murine C26 colon carcinoma cells (accession: GSE24112).[17] In this study, mice were divided into normal control, moderate cachexia (10% loss of baseline body mass), and severe cachexia (15% loss of body mass). There was no significant difference in the examined genes from the adaptive immune system (*Figure* 1A). However, there was a significant difference in the tryptase alpha/beta 1 (TPSAB1) and Cluster of Differentiation 68 (CD68) genes from the innate immune system (*Figure* 1B). TPSAB1 and tryptase beta 2 (TPSB2) are commonly associated with mast cells.[37] CD68 is commonly used as a macrophage marker.[38] Closer inspection of each of the genes showed significantly increased expression of TPSAB1 in the muscle of cachectic mice compared with the corresponding normal control mice (*Figure* 1C), and there was also an observed trend toward increased TPSB2 expression in early cachectic mice compared with control (*Figure* 1D). Additionally, CD68 expression was significantly increased in the severe cachexia mice compared with normal control mice (*Figure* 1E). Collectively, these data suggest the innate immune cells, such as mast cells and macrophages, are accumulated in the skeletal muscles derived from mice with cancer-associated cachexia.

Subcutaneous LL/2 injection induces cachexia in vivo

The LL/2 subcutaneous injection model is one of the most well-established murine cancer-associated cachexia models currently in use to induce loss of muscle mass and function.[39–41] Therefore, LL/2 cells were inoculated subcutaneously into C57BL/6 mice to establish cancer-associated cachexia. The tumour-free body mass of the LL/2-bearing mice at the time of harvest was significantly lower than corresponding sham mice (*Figure* 2A). However, there was no significant difference in daily food intake between the groups, indicating that a change in diet is not responsible for the weight loss (*Figure* 2B). There was a trend toward higher percentage loss of body mass correlating with increased tumour size (*Figure* 2C). To assess if loss of muscle mass specifically was contributing to this loss in body mass, the primarily fast twitch fibre EDL, predominantly slow twitch fibre SOL, and mixed fibre type GA and TA muscles were excised and weighed.[40,42] In this case, to further assess correlations between the reduction of body weight and the reduction of muscle weight, LL/2-bearing mice were stratified further into mice losing less than 10% [LL/2 ($<$10%)] and 10% or greater [LL/2 ($\geq$10%)] of their baseline (pre-inoculation) body mass. Significant decreases in individual excised muscle mass of the TA (*Figure* 2D) and GA muscles (*Figure* 2E) in LL/2 ($\geq$10%) mice were observed compared with sham, indicative of muscle wasting. There were slight trends toward decreased mass in the EDL (*Figure* 2F) and SOL muscles (*Figure* 2G), although this did not reach statistical significance. Furthermore, muscle function was examined using an *in vivo* force transducer system to measure force frequency following electrode stimulated plantarflexion.[31] There was a significant decrease in force frequency in measurements taken in LL/2 ($\geq$10%) mice compared with sham in measurements taken just prior to harvest (*Figure* 2H), and a trend toward decreased time to muscle fatigue (*Figure* 2I).

A

Gene	ILMN ID#	Adaptive Immunity	Summary P Value
CD19	2975994	B Cells	0.3594
CD3D	2697415	T Cells	0.4321
CD3G	2722784	T Cells	0.6233
CD8	2664929	Cytotoxic T Cells	0.9938
CD4	1249663	Helper T Cells	1.0000

B

Gene	ILMN ID#	Innate Immunity	Summary P Value
TPSAB1	2705860	Mast Cells, Basophils	0.0018
CD68	2689785	Macrophages, Monocytes	0.0167
TPSB2	3161036	Mast Cells	0.0557
CD14	2742075	Macrophages, Neutrophils	0.1907
CD86	1217041	Antigen Presenting Cells	0.2026
CD123	2916571	Basophils, GMPs	0.3110
Ly6G	2697910	Neutrophils, Monocytes	0.3314
CD80	2877958	Antigen Presenting Cells	0.5797
NK1.1	2952650	NK Cells	0.5799

GMPs: Granulocyte-Monocyte Progenitor Cells

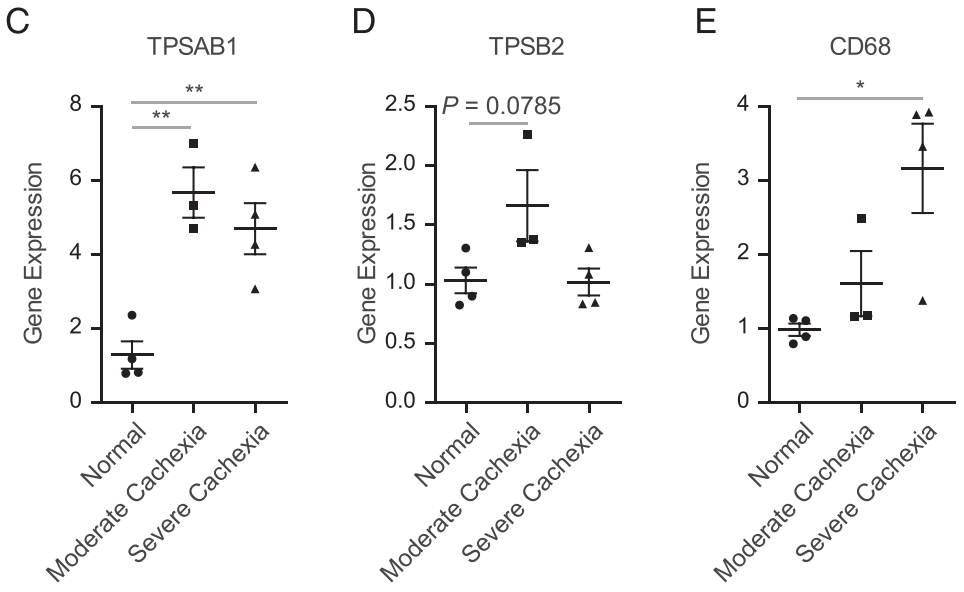

Figure 1 Increased expression of innate immune cell genes in cachectic mice skeletal muscle. (*A*) Expression of adaptive immunity-related genes in quadriceps muscles of C26 colon carcinoma-bearing mice [GSE24112, normal (n = 4), moderate cachexia (n = 3), and severe cachexia (n = 4)]. (*B*) Expression of innate immunity-related genes. Detailed analyses of (*C*) tryptase alpha/beta 1 (TPSAB1), (*D*) tryptase beta 2 (TPSB2), and (*E*) CD68 gene expression from (B). Mean ± SEM. $^{*}P \leq 0.05$, $^{**}P \leq 0.01$ (one-way ANOVA, Tukey's multiple comparisons test).

Individual muscle fibres from each of the excised muscle tissues were visualized using Wheat Germ Agglutinin to further analyse changes in muscle fibre sizes (*Figure* 3A). Quantification of the distribution of fibre sizes within each muscle showed a significant shift toward a higher frequency of small muscle fibres in the TA (*Figure* 3B) and

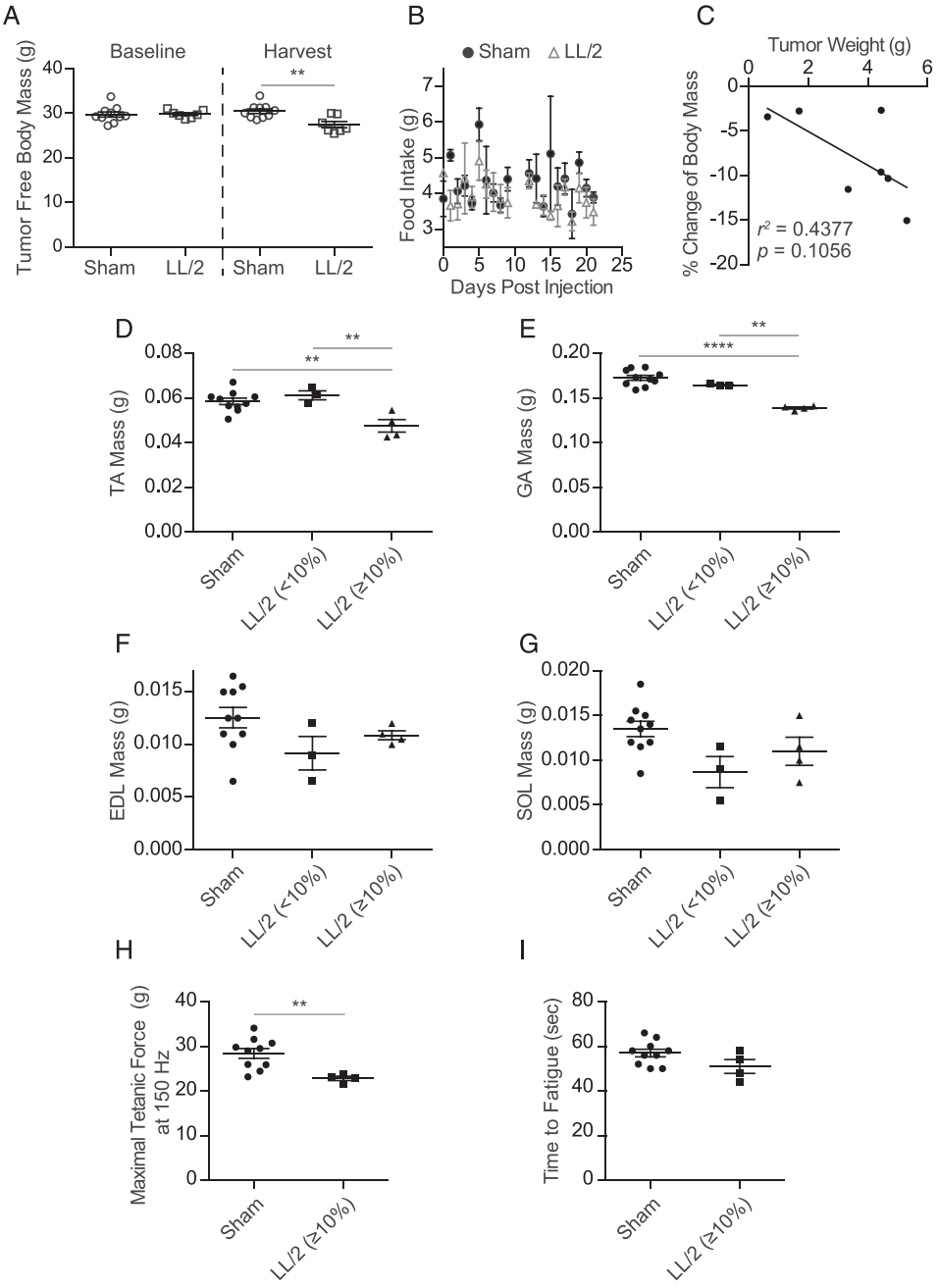

Figure 2 Murine model of LL/2 induced cachexia. Murine lung cancer LL/2 cells or cell culture medium without cells (sham) were inoculated into C57BL/6 mice subcutaneously (sham n = 10, LL/2 n = 7). Body weight, food intake, tumour growth, and muscle function were assessed after 3 weeks. (*A*) Tumour free body mass of LL/2 and sham-bearing mice at baseline and termination of experiment. (*B*) Longitudinal measurement of daily food intake of LL/2 and sham-bearing mice. (*C*) Correlative comparison of excised tumour mass with percentage of body mass lost. (*D–G*) Comparison of muscle mass among sham-bearing mice and LL/2 bearing mice losing <10% or ≥10% baseline body mass at termination of experiment. Mean ± SEM, $^{**}P \leq 0.01$, $^{****}P \leq 0.0001$ vs. sham-injected group (one-way ANOVA, Bonferroni's multiple comparisons test). (*H, I*) Hind limb muscle function [(H) maximal tetanic force and (I) time to fatigue] was measured by force transduction at termination of experiment. Mean ± SEM, $^{**}P \leq 0.01$ vs. sham-injected group (Student's *t*-test).

GA (*Figure* 3C) in LL/2 (≥10%) mice, compared with the sham control. A similar trend was seen in the EDL muscle, although this did not reach statistical significance (*Figure* 3D). However, the SOL tissue did not show a significant change in fibre size distribution (*Figure* 3E). This is potentially due to fast-twitch muscle fibres being predominantly affected in cancer cachexia.[43] Interestingly, mRNA expression of the muscle protein specific E3 ubiquitin ligases

DOI: 10.1002/jcsm.12714

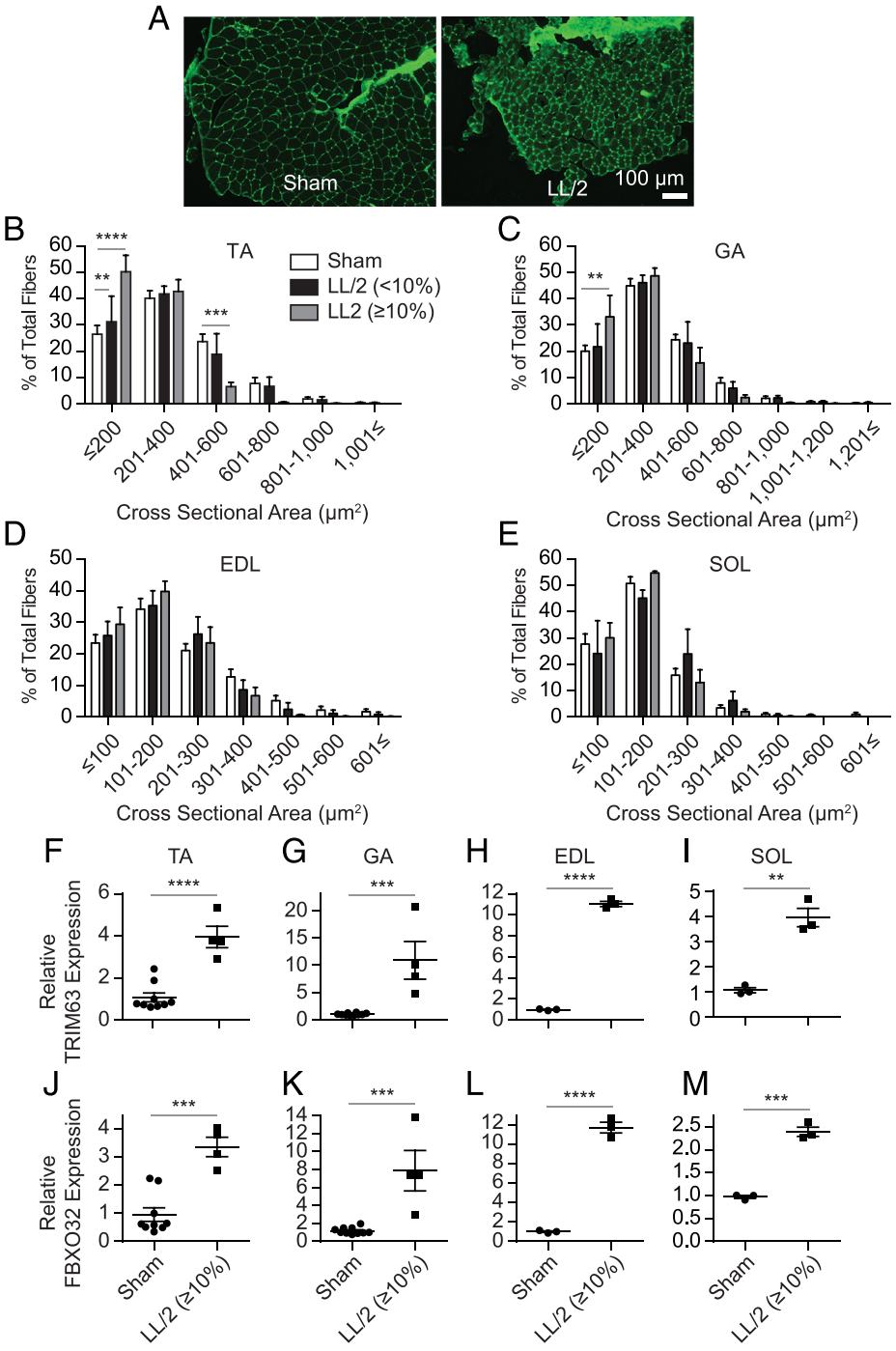

Figure 3 Cachexia shifts muscle fibre size distribution and increases cachexia-related genes in *in vivo* murine model. Analysis of muscle fibre cross-sectional area and cachexia-related gene expression in muscles obtained from animals in *Figure*2. (*A*) Representative images of wheat germ agglutinin (WGA) stained TA muscles. ×10. Bar = 100 µm. (*B–E*) Quantification of muscle fibre cross-sectional area percent distribution. Mean ± SEM, $^{**}P \leq 0.01$, $^{***}P \leq 0.001$, $^{****}P \leq 0.0001$ vs. sham-injected group (two-way ANOVA, Tukey's multiple comparisons test). (*F–I*) tripartite motif containing 63 (TRIM63) and (*J–M*) F-box protein 32 (FBXO32) mRNA expression of muscles. Mean ± SEM. $^{**}P \leq 0.01$, $^{***}P \leq 0.001$, $^{****}P \leq 0.0001$ vs. sham-injected group (Student's *t*-test).

tripartite motif containing 63 (TRIM63) and F-box protein 32 (FBXO32), which have previously been shown to be up-regulated in cancer-associated cachexia,[44,45] were significantly increased in all of the skeletal muscles of LL/2 (≥10%) mice compared with the sham control. Together, these findings suggest mice that lost 10% or greater of their weight are representative of a cancer-associated cachexia phenotype.

Cachectic mice have increased degranulating skeletal muscle mast cells, but not macrophages and neutrophils

In order to assess the presence of innate immune cells in this model, skeletal muscle tissue was examined for resident mast cells, macrophages, and neutrophils within the endomysium and perimysium. The presence of mast cells within the skeletal muscle was visually confirmed using toluidine blue stain (*Figure* 4A). Mast cells naturally resided in the skeletal muscle of both sham control and LL/2-bearing mice. The total number of mast cells per muscle cross section was quantified, and there was a significant increase of the total number of mast cells in the EDL tissue of LL/2 (≥10%) mice (*Figure* 4B–E). Degranulation, or granule release, of activated mast cells was assessed using the morphology of the mast cells.

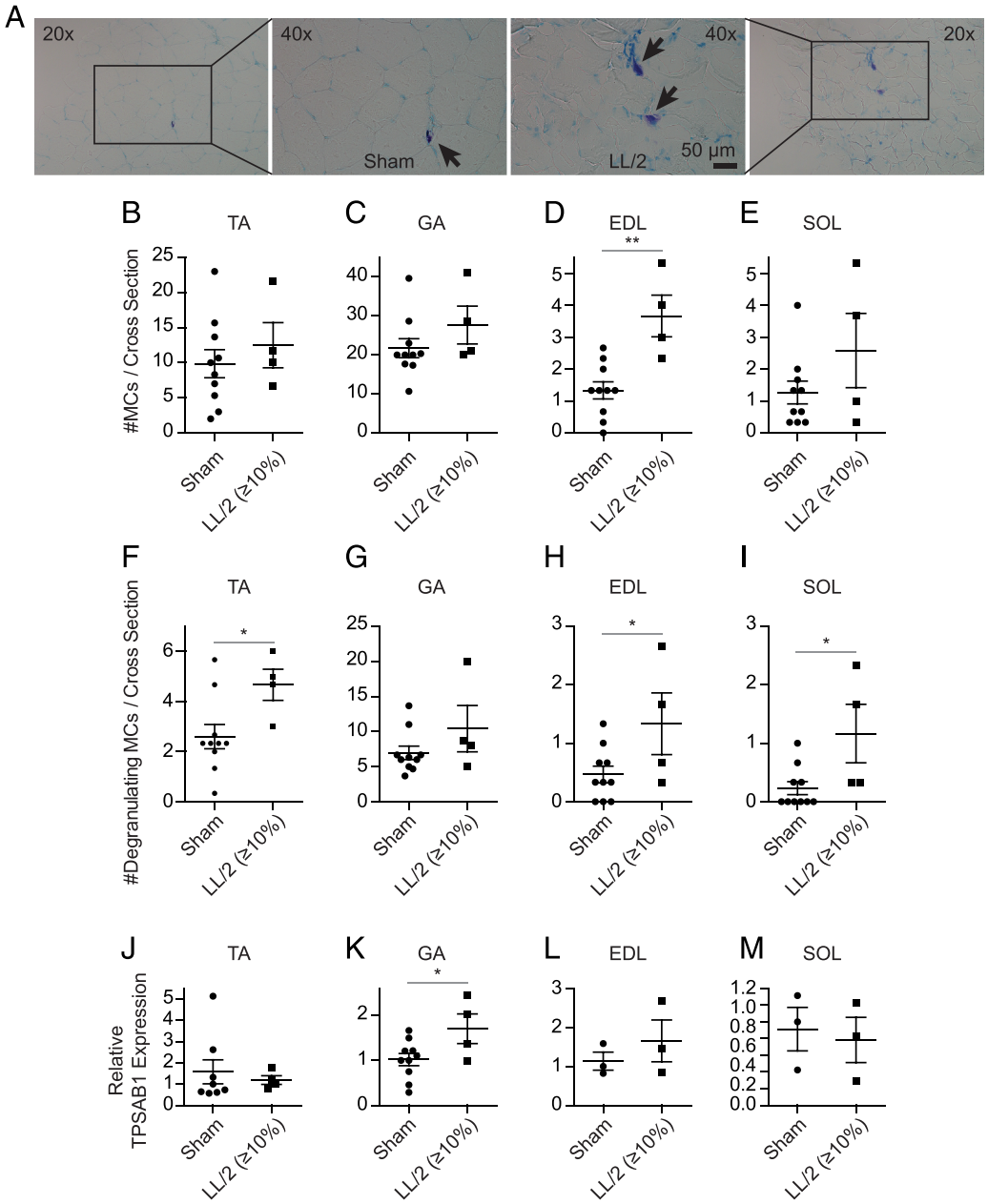

Figure 4 Degranulating skeletal muscle-resident mast cells increase in *in vivo* murine cancer-associated cachexia model. Examination of skeletal muscle-resident mast cells (MCs) in muscles obtained from animals in *Figure*2. (*A*) Representative images of toluidine blue stained TA muscle. ×20 and ×40. Bar = 25 μm. (*B–I*) Quantification of total number of muscle-resident (*B–E*) mast cells and (*F–I*) activated degranulating mast cells in hind limb skeletal muscles. (*J–M*) Relative mRNA expression of tryptase alpha/beta 1 (TPSAB1) in the muscles. Mean ± SEM, $^{*}P \leq 0.05$, $^{**}P \leq 0.01$ vs. sham-injected group (Student's *t*-test).

Interestingly, there was a significant increase in the number degranulating mast cells within the EDL, TA, and SOL tissue, and a trend toward increased degranulating mast cells in the GA of LL/2 (≥10%) mice, compared with the sham mice (*Figure* 4F–I). Relative TPSAB1 mRNA expression was also assessed in each of these muscle tissues (*Figure* 4J–M). Only a significant difference was observed in the GA muscle (*Figure* 4K), potentially due to the larger number of mast cells present within this larger muscle compared with the other smaller muscles measured.

CD68 (*Figure* 5A) and neutrophil elastase (NE) positive staining (*Figure* 5J) were quantified as representative markers for macrophages and neutrophils, respectively, within the skeletal muscle tissue. However, within this model, skeletal muscle-resident macrophages (*Figure* 5B–E) and neutrophils (*Figure* 5K–N) were not upregulated in the cachectic TA, GA, EDL, and SOL muscles. Relative mRNA expressions of the corresponding genes for these markers were also assessed in each muscle of interest. There was a significant increase in CD68 expression in the SOL of LL/2 (≥10%) mice (*Figure* 5I), but not in the TA, GA, and EDL muscles (*Figure* 5F–H). Relative mRNA expression of the neutrophil elastase gene (ELANE) showed no significant difference in the TA (*Figure* 5O), significantly lower levels in the EDL of LL/2 (≥10%) mice (*Figure* 5Q), and significantly higher levels in the GA and SOL muscles (*Figure* 5P & R).

Next, to examine if the gene expression changes observed in *Figures* 3–5 corresponded with changes in protein expression, Western blot assays were performed on the excised muscles. There was a significant increase in mast cell-specific protease tryptase expression in the TA of LL/2 (≥10%) mice, but not in the GA, EDL, and SOL muscles (*Figures* 6A–D & 7A). While tryptase remains a well-established component of mast cell granules, typically mast cells are heterogeneous and may or may not produce tryptase,[46] which may partially explain why degranulating mast cells from different muscles also differ in tryptase protein expression. Additionally, upon degranulation tryptase may enter the circulation, thus serum levels may be needed in future studies to fully assess changes in tryptase protein expression.[47] No change was observed in mast cell surface protein Mas-related gene X2 (MrgX2) levels in all four muscle types (*Figures* 6A–D & 7B), suggesting again that the activation status of mast cells may be changing, while the total number of mast cells remains the same. CD68 protein expression showed significantly lower levels in the TA of LL/2 (≥10%) mice (*Figures* 6A & 7C), and significantly higher levels in the GA (*Figures* 6B & 7C). There was a significant increase in MPO, an enzyme found in neutrophils, expression in the TA, EDL, and SOL of LL/2 (≥10%) mice (*Figures* 6A, C, & D & 7D), but not in the GA (*Figures* 6B & 7D**)**. Although there were significant increases of mRNA expression of the muscle protein specific E3 ubiquitin ligases TRIM63 and FBXO32 in all of the skeletal muscles of LL/2 (≥10%) mice (*Figure* 3F–M), there were no significant increases in the expression of muscle-specific RING finger-1 (MuRF1, protein for TRIM63) and muscle atrophy F-box (MAFbx, protein for FBXO32) (*Figures* 6A–D & 7E & F), suggesting that muscle degradation through the muscle protein specific E3 ubiquitin ligases may not be the sole mechanism of muscle atrophy observed in our study. Moreover, there were no significant changes in fast myosin skeletal heavy chain (MyHC), known to be decreased in cancer-related cachectic muscles,[10,48] protein expression (*Figures* 6A–D & 7G). However, some reduction of MyHC levels were observed in TA and GA muscles of LL/2-bearing mice, which show significant muscle wasting (*Figures* 2D & E & 3B & C), although this reduction did not reach statistical significance (*Figures* 6A & B & 7G). This is consistent with recent findings that MyHC may not be selectively decreased in murine cancer cachexia,[49] and that other insults (e.g. denervation) are necessary to develop MyHC loss in cancer-associated cachectic muscles.[50] Although further studies are clearly warranted, this may be one reason that we did not observe significant reduction of MyHC protein levels at the time of harvest.

Collectively, the histology data indicate an overall increase in the number of degranulating mast cells, but not $CD68^+$ and NE^+ cells in the skeletal muscle of cancer-associated cachectic mice, while western blot analysis shows some increase of tryptase, CD68, and MPO protein levels in those muscles.

Cancer cell secretome activates mast cells

To next address the ability of secreted factors from cachexia-inducing cancer cells to activate mast cells, mast cells were treated with CM from the LL/2 cell line. LL/2 CM up-regulated lysosome-associated membrane protein 2 (LAMP2) expression in the P815 mastocytoma cell line relative to control following 10 min of stimulation (*Figure* 8A). This up-regulation occurs when mast cells are activated to degranulate.[33] Primary BMMC released significantly higher levels of IL-6 in the media 24 h post-stimulation with LL/2 CM compared with IL-6 levels of BMMC or LL/2 CM alone, indicative of mast cell activation (*Figure* 8B). Differentiated C2C12 murine myotubes treated with media from LL/2-pre-activated mast cells showed significantly reduced myotube diameter at 24 h post-treatment compared with C2C12 myotubes treated with fresh growth media (Control CM), LL/2 CM, or BMMC CM (*Figure* 8C). To further determine whether the observed reduction of myotube diameter mediated by BMMC-derived CM were associated with muscle atrophy, MyHC levels in C2C12 myotubes were compared. Interestingly, similar trends were observed in changes in MyHC expression as those in myotube diameter reduction observed in *Figure* 8C, although it did not reach statistical significance (*Figure* 8D & E). This trend is also similar to MyHC level changes observed in TA and GA muscles of LL/2-bearing mice (*Figures* 6A & B & 7G) which show significant muscle

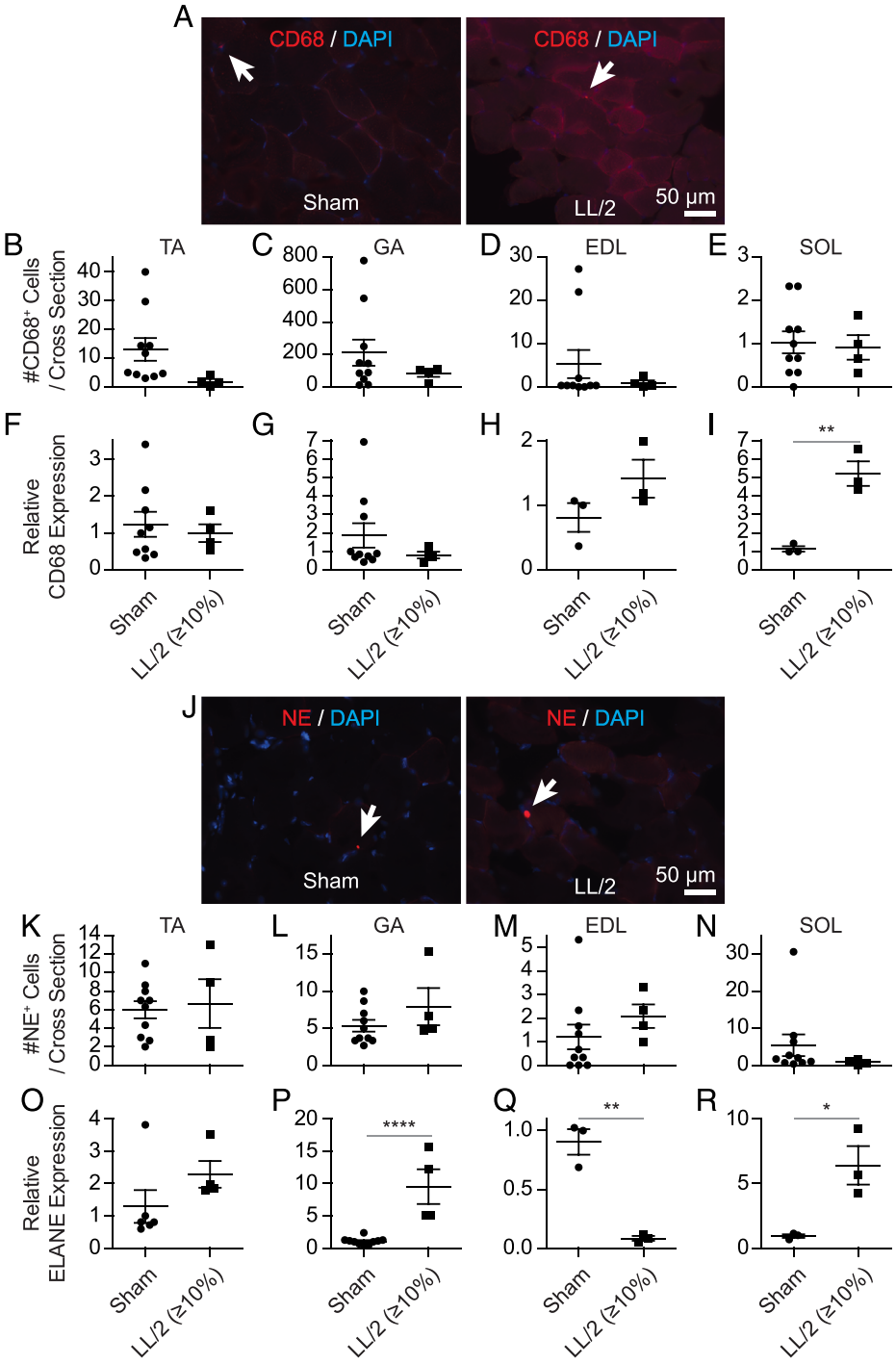

Figure 5 No change in skeletal muscle-resident macrophages and neutrophils in murine cancer-associated cachexia model. Examination of skeletal muscle-resident CD68 (macrophage marker) positive cells and neutrophil elastase (NE) (neutrophil marker) positive cells in muscles obtained from animals in *Figure*2. (*A*) Representative immunofluorescence images of CD68 and DAPI stained TA muscle. ×20. Bar = 50 μm. (*B–E*) Quantification of number of positive CD68 cells per muscle cross section. (*F–I*) Relative mRNA expression of CD68 in muscle. (*J*) Representative immunofluorescence images of NE and DAPI stained TA muscle ×20. Bar = 50 μm. (*K–N*) Quantification of number of positive NE cells per muscle cross section. (*O–R*) Relative mRNA expression of neutrophil elastase gene (ELANE) in muscle. Mean ± SEM. $^{*}P \leq 0.05$, $^{**}P \leq 0.01$, $^{****}P \leq 0.0001$ vs. sham-injected group (Student's *t*-test).

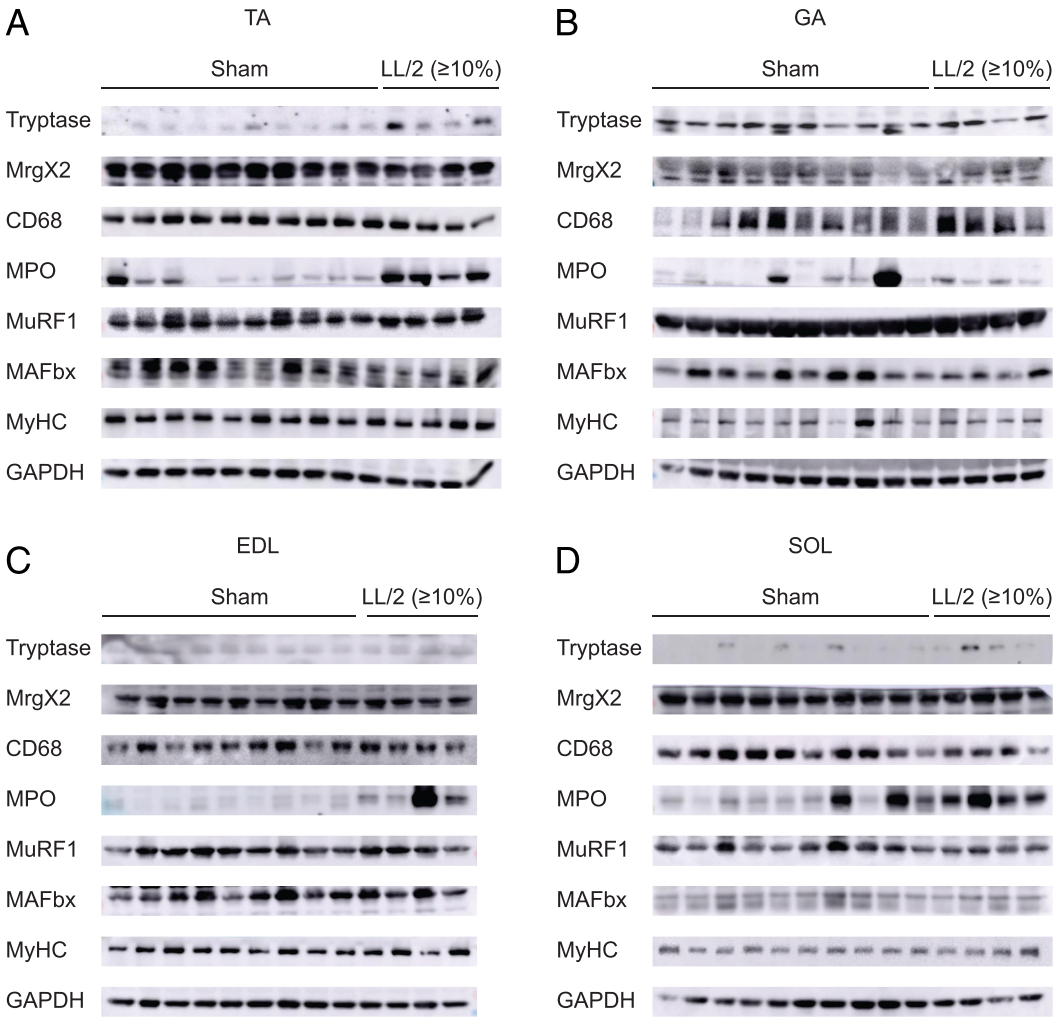

Figure 6 LL/2 altered expression of innate immune cell markers in skeletal muscles, but did not affect protein expression of muscle protein specific E3 ubiquitin ligases. Representative western blot of tryptase, Mas-related gene X2 (MrgX2), CD68, myeloperoxidase (MPO), muscle-specific RING finger-1 (MuRF1), muscle atrophy F-box (MAFbx), and fast myosin skeletal heavy chain (MyHC) on (*A*) TA, (*B*) GA, (*C*) EDL, and (*D*) SOL muscles obtained from animals in *Figure*2. GAPDH was used for loading control.

wasting (*Figures* 2D & E & 3B & C). LL/2 cells release factors into their secretome that initiate measurable levels of mast cell activation and degranulation *in vitro*. In turn, activated mast cell media has a direct effect on myotube fibre size, suggesting that cancer-activated mast cells may promote the progression of the characteristic muscle atrophy in cachexia.

Mast cell signatures up-regulated in cachectic skeletal muscle

To address the translational potential of our findings in humans and evaluate the efficaciousness of mast cells as a cachexia biomarker and mediator in humans, we first assessed the correlation between cachexia-related signatures and innate immune cell signatures in human skeletal muscle tissue. Publicly available signatures for mast cells, neutrophils, and macrophages had a significant positive correlation with both skeletal muscle atrophy (*Figure* 9A–C) and apoptosis (*Figure* 9D–F), dietary excess/increased energy expenditure (*Figure* 10A–C), and cachexia (*Figure* 10D–F) signatures in normal skeletal muscle tissue samples from the Genotype-Tissue Expression project.[22–26,28,29] To examine if these immune signatures were also enriched in cachectic muscle tissue, gene set enrichment analysis was used with publicly available human cohorts of upper GI cancer and pancreatic ductal adenocarcinoma (PDAC).[24,27] In the upper GI cancer cohort, patient quadriceps muscle biopsies were divided into normal control samples, and PreOp samples from upper GI cancer patients scheduled for tumour resection with a 7% body mass loss (accession: GSE 34111).[20] The primary criteria considered for evaluating enrichment significance were: (i) a positive normalized enrichment score (NES), (ii) a false discovery rate below 0.1, and (iii) a family-wise error rate below 0.05. Using this

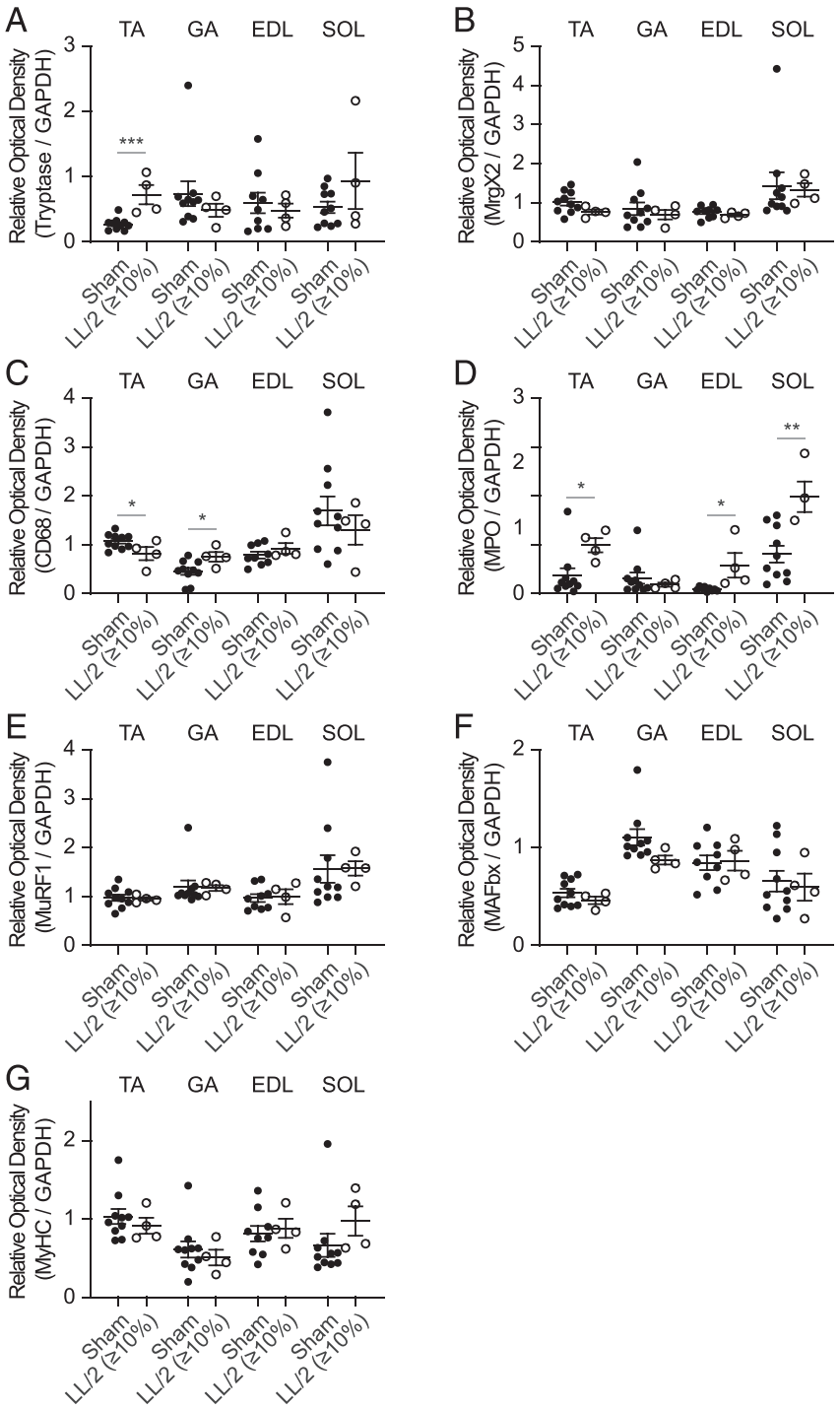

Figure 7 LL/2 altered expression of innate immune cell markers in skeletal muscles, but did not affect protein expression of muscle protein specific E3 ubiquitin ligases. Quantifications of western blots in *Figure* 6. (*A*) tryptase, (*B*) Mas-related gene X2 (MrgX2), (*C*) CD68, (*D*) myeloperoxidase (MPO), (*E*) muscle-specific RING finger-1 (MuRF1), (*F*) muscle atrophy F-box (MAFbx), and (*G*) fast myosin skeletal heavy chain (MyHC). Mean ± SEM. $^{*}P \leq 0.05$, $^{**}P \leq 0.01$, $^{***}P \leq 0.001$ vs. sham-injected group (Student's *t*-test).

criterion, there was no significant enrichment in gene signatures for adaptive immunity, macrophages, or neutrophils in the cachectic PreOp samples (*Figure* 11A, D, & E); however, there was enrichment of both the innate immunity and mast cell signatures (*Figure* 11B & C). The PDAC cohort contained rectus abdominis muscle biopsy samples from both cachectic and non-cancer bearing patients (GSE130563).[21,30] In this cohort, the greatest enrichment and lowest false discovery rate

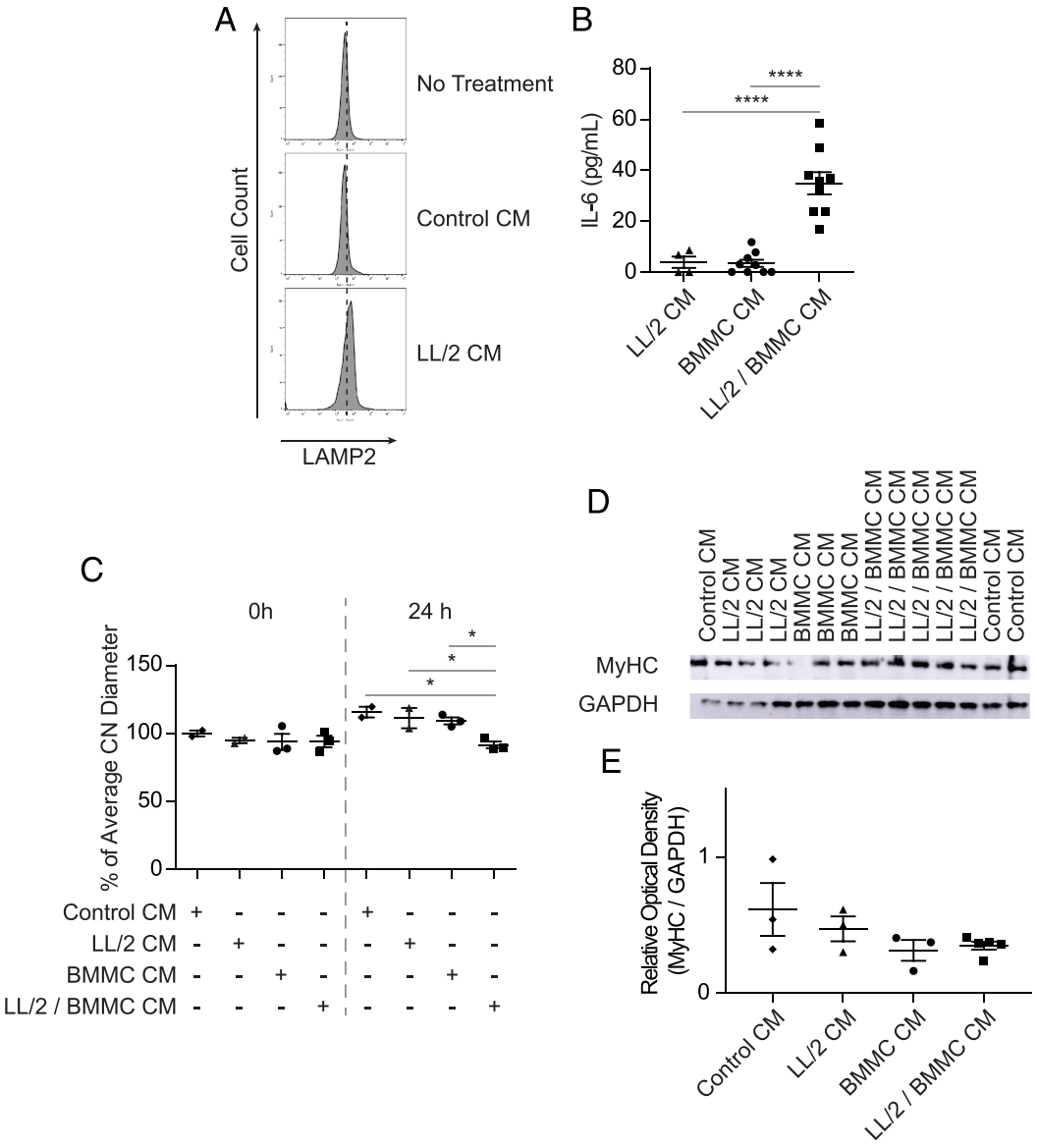

Figure 8 LL/2 activated mast cells decrease differentiated Myotube diameter. (*A*) Representative histogram of LAMP2 expression in P815 cells with no treatment, control conditioned media (CM), or LL/2 CM. (*B*) IL-6 levels at 24 h in (i) LL/2 CM, (ii) bone marrow-derived MC (BMMC) CM, and (iii) BMMC CM treated with LL/2 CM (LL/2 / BMMC CM). Mean ± SEM. $^{****}P \leq 0.0001$ (one-way ANOVA, Tukey's multiple comparisons test). (*C*) Differentiated murine C2C12 myotubes were treated with (i) control CM, (ii) LL/2 CM, (iii) BMMC CM, or (iv) LL/2/BMMC CM for 24 h. The average C2C12 myotube diameter was measured under the microscope. Mean ± SEM. $^{*}P \leq 0.05$ (one-way ANOVA, Tukey's multiple comparisons test). (*D*) Representative western blot of fast myosin skeletal heavy chain (MyHC) expression in differentiated murine C2C12 myotubes treated with (i) control CM, (ii) LL/2 CM, (iii) BMMC CM, or (iv) LL/2/BMMC CM for 24 h. (*E*) Quantification of western blot in *Figure*8D. Mean ± SEM. (one-way ANOVA, Tukey's multiple comparisons test).

was seen in the mast cell signature (*Figure* 11H), compared with the adaptive immunity, innate immunity, macrophage, and neutrophil signatures (*Figure* 11F, G, I, & J). The enrichment of this mast cell signature within muscle biopsies of cancer-associated cachectic patients from two separate cancer types suggests that skeletal-resident mast cells are enriched in the muscles of cancer-associated cachexia patients.

Discussion

This study sought to identify and assess the potential efficacy of skeletal-muscle resident immune cells as mediators and/or biomarkers for cancer-associated cachexia. Using a publicly available murine bioinformatics cohort, individual innate and adaptive immune cell genes in a murine C26 model of cachexia revealed significant changes only in innate immune

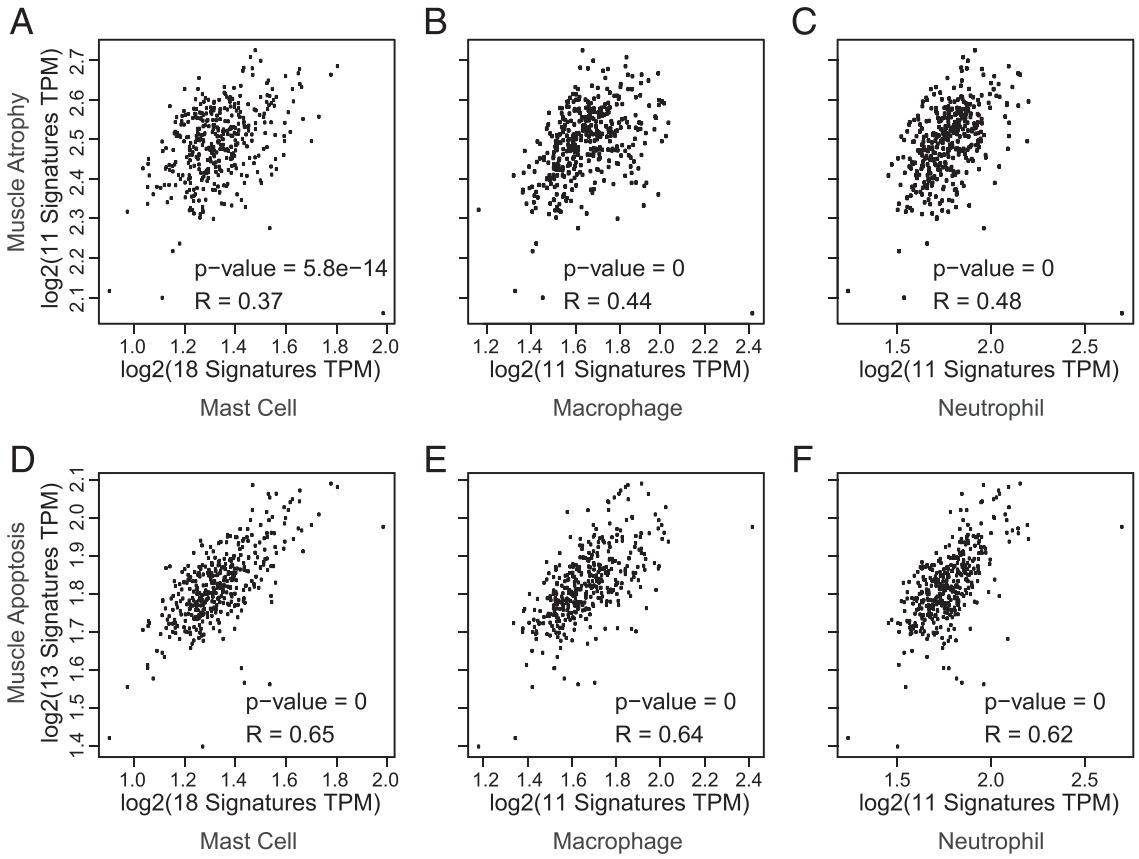

Figure 9 Innate immune cell signatures positively correlate with skeletal muscle atrophy and apoptosis signatures. Spearman's correlation of muscle atrophy gene signature and (*A*) mast cell, (*B*) macrophage, and (*C*) neutrophil gene signatures in human skeletal muscle tissue from the genotype-tissue expression (GTEx) project. Correlation of muscle apoptosis signatures and (*D*) mast cell, (*E*) macrophage, and (*F*) neutrophil gene signatures.

cell genes.[17–19] This finding prompted a focus on innate immune cells in an *in vivo* LL/2 model for cancer-associated cachexia. The development of cachexia in the immunocompetent C57BL/6 mice coincided with an increased number of activated and degranulating skeletal muscle-resident mast cells, as shown through toluidine blue staining. However, immunofluorescence staining for macrophages and neutrophils showed no significant difference in the skeletal muscle. To determine the effect of LL/2-activated degranulating mast cells on muscle cells in a controlled *in vitro* setting, C2C12 myotubes were treated with LL/2-pre-activated BMMC CM and decreased myotube diameter was observed after 24 h. With the observations from the murine bioinformatics cohort, *in vivo* LL/2 model, and *in vitro* C2C12 experiments indicating a potential role for mast cell activation in the progression of cancer-associated cachexia, publicly available human cohorts were assessed to determine the translational potential of these findings. While immune response signatures for mast cells, macrophages, and neutrophils all positively correlated with signatures for muscle apoptosis and atrophy, dietary excess, and cachexia signatures in normal skeletal muscle tissue, only the mast cell signature was enriched in both the cachectic patients of the upper GI cancer and PDAC cohorts.[18–29] These findings suggest that activated skeletal-muscle resident mast cells are enriched in the cachectic muscles. Therefore, skeletal-muscle resident mast cells may serve as a biomarker and mediator for cancer-associated cachexia.

It is well established that inflammatory factors are key in the development of cancer-associated cachexia, and the exact sources of this inflammation have remained a focus of study in the cachexia field.[1] Mast cells are one established producer of the well characterized pro-cachectic cytokine IL-6,[13] and as evidenced in our *in vivo* and *in vitro* experiments are activated directly by the cachexia-inducing LL/2 cell secretome. While little is known about the effects of skeletal muscle-resident mast cell accumulation and activation on skeletal muscle tissue in cancer-associated cachexia patients, there are multiple instances of mast cell promoted muscle atrophy occurring in other conditions. For example, elevated numbers of degranulating skeletal muscle-resident mast cells have been previously implicated in the development of the autoimmune myopathy polymyositis[15] and Duchenne muscular dystrophy.[16] Another recent study observed increased

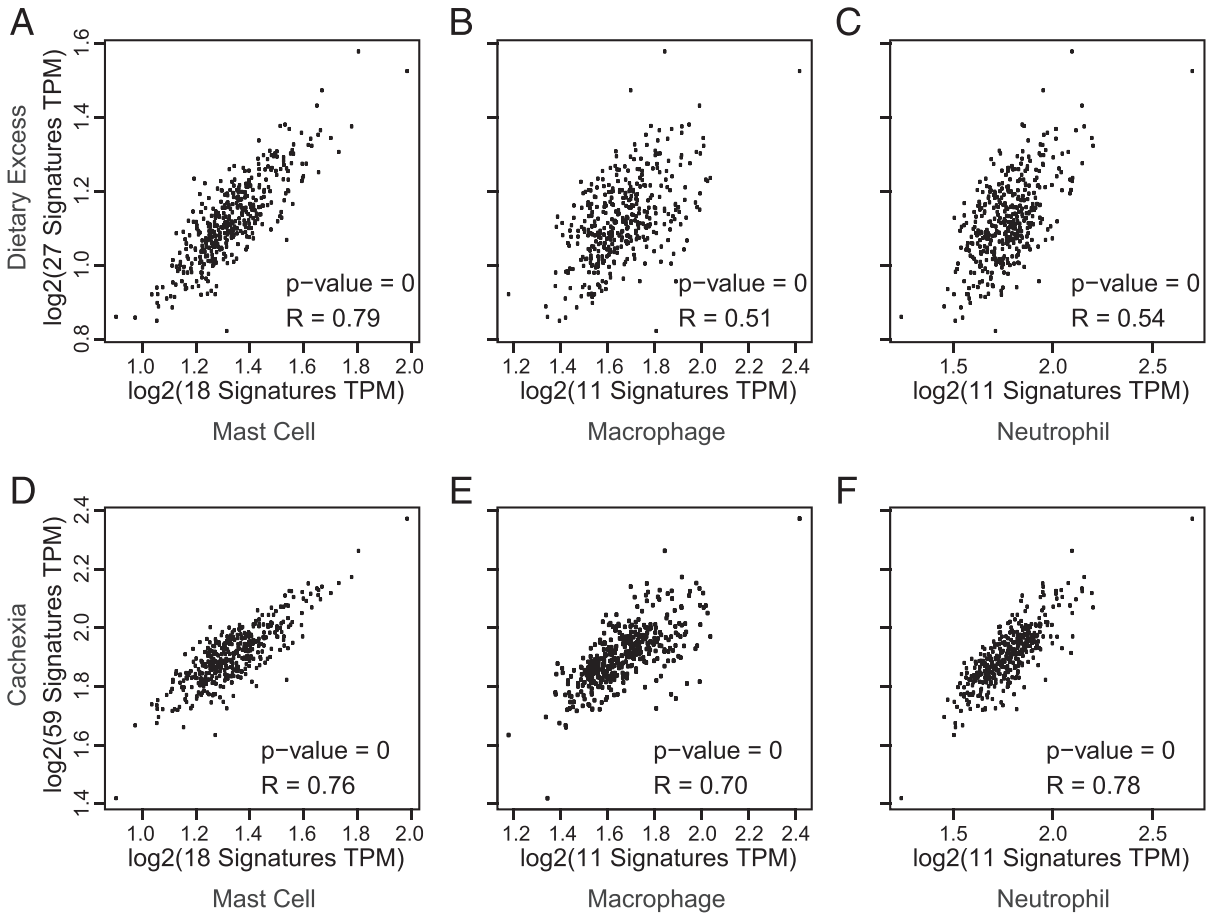

Figure 10 Innate immune cell signatures positively correlate with dietary excess and cachexia signatures. Spearman's correlation of dietary excess gene signature and (*A*) mast cell, (*B*) macrophage, and (*C*) neutrophil gene signatures in human skeletal muscle tissue from the genotype-tissue expression (GTEx) project. Correlation of cachexia signatures and (*D*) mast cell, (*E*) macrophage, and (*F*) neutrophil gene signatures.

levels of mast cells, many with a degranulating phenotype, in the quadriceps muscle of amyotrophic lateral sclerosis patients.[51] These cases establish a clear precedent of skeletal-muscle resident mast cell numbers and activation increasing in conditions resulting in skeletal muscle atrophy. Furthermore, the results from these muscle atrophy studies are mirrored in our own findings, where cancer-associated cachexia: (i) increased the number of activated degranulating skeletal muscle-resident mast cells in murine hind limb muscles and (ii) increased a mast cell mediated immunity signature in cachectic patient samples.

Although a potential key player in the characteristic inflammation observed in this condition, skeletal muscle-resident mast cells may not be the sole inducer of cancer-associated cachexia and all of its systemic effects. There may be other immune cells simultaneously at play throughout the various tissues affected in cancer-associated cachexia. For example, macrophages are upregulated in the colon of cachectic colon cancer patients.[52] However, within the skeletal muscle tissue specifically, mast cell activation was the most consistently observed innate immune cell up-regulation across the murine and patient samples (both upper GI cancer and PDAC) in this study. It is worth noting that other immune cells may also be up-regulated dependent upon the cancer type and immune cell markers used for identification. For example, $CD163^+$ macrophages, or M2 macrophages, were up-regulated in the skeletal muscle of cachectic PDAC patients in a recent study,[53] while we observed a statistically insignificant enrichment in cachectic PDAC patients and no enrichment in cachectic upper GI cancer patients using a macrophage immune response gene signature. Additionally, the C26 mouse bioinformatics cohort (GSE24112) showed an up-regulation in CD68 expression in the skeletal muscle, while our *in vivo* studies with LL/2 showed no significant increase in skeletal muscle-resident $CD68^+$ cells and only slightly increased CD68 protein in GA muscle tissues. This contradiction may be due to inherent differences in the colon carcinoma and lung cancer models or in the examined muscles (e.g. quadriceps vs. GA). Furthermore, we observed significant increases of MPO protein expression in TA, EDL,

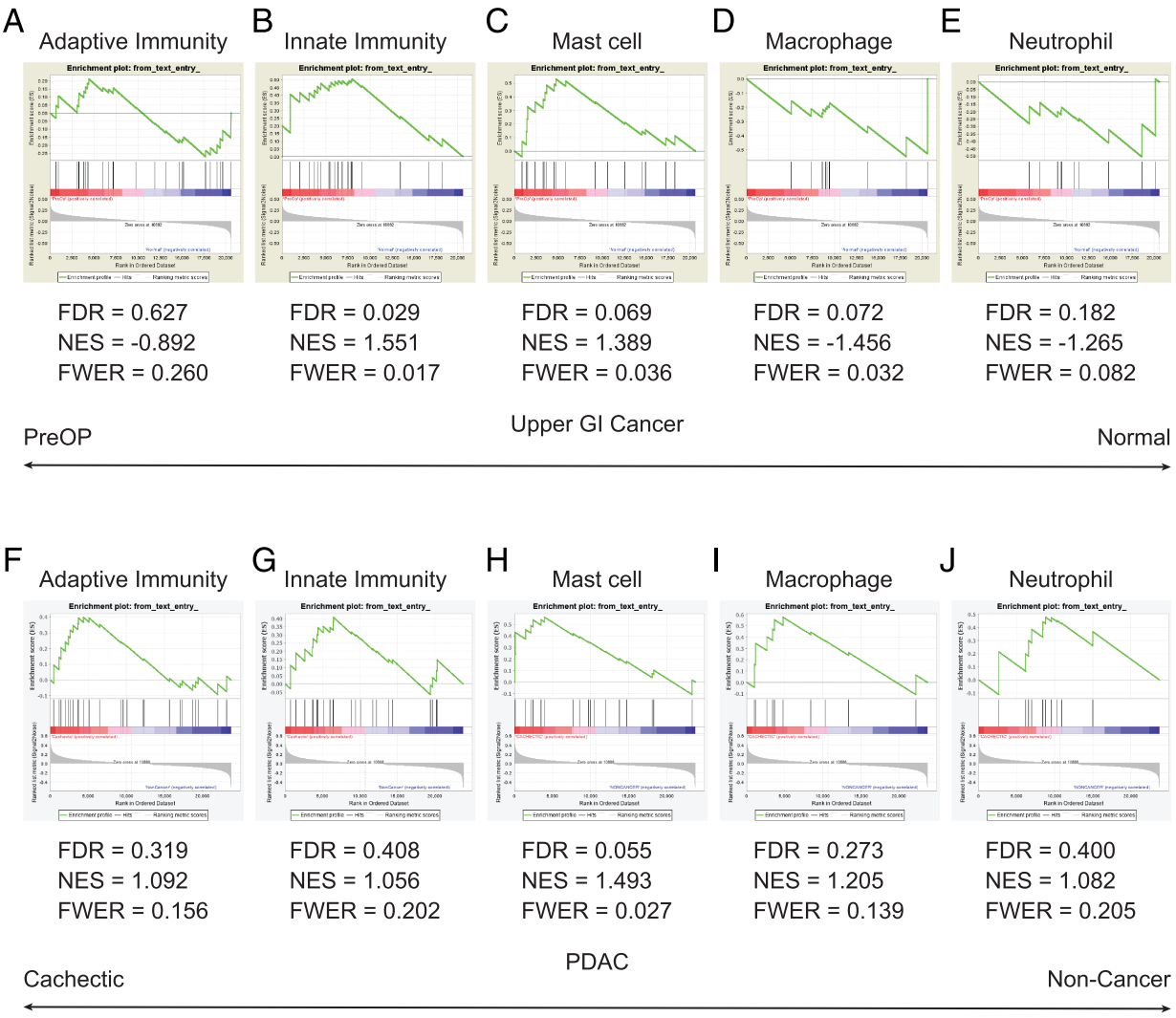

Figure 11 Enriched mast cell gene signature in muscles of cachectic upper GI cancer and PDAC patients. Gene set enrichment analyses of (*A*) adaptive immunity, (*B*) innate immunity, (*C*) mast cell, (*D*) macrophage, and (*E*) neutrophil gene signatures expressed in the quadriceps muscles obtained from upper gastrointestinal (GI) cancer patients from GSE34111 with 7% weight loss (n = 12, PreOp) and normal controls (n = 6, normal). Enrichment plots of (*F*) adaptive immunity, (*G*) innate immunity, (*H*) mast cell, (*I*) macrophage, and (*J*) neutrophil gene signatures expressed in the rectus abdominis muscles obtained from pancreatic ductal adenocarcinoma (PDAC) patients from GSE130563 with cachexia (n = 17, cachectic) or non-cancer controls (n = 16, non-cancer). FDR, false discovery rate; NES, normalized enrichment score; FWER, family-wise error rate.

and SOL muscles, while there was no change in the number of NE^+ cells in those muscles. Because MPO is known to be a potent and selective inhibitor of mast cell tryptase,[54] some compensatory mechanisms may be initiated to mitigate the impact of skeletal muscle-resident mast cells on muscle wasting, resulting in upregulation of this protein. Further studies are clearly required to determine the full efficacy and penetrance of skeletal muscle-resident mast cell activation as a biomarker and mediator for cancer-associated cachexia in patients across multiple cancer types and stages, as cachexia is a complex and variable condition.[4] For a less invasive diagnostic strategy, it would also be prudent to evaluate levels of activated mast cell released factors such as tryptase and heparin in the serum of cancer cachexia patients in future studies.[55,56] Still, the addition of skeletal muscle-resident activated mast cells as a biomarker has the potential to enhance identification of at-risk cancer patients.

Cancer-associated cachexia is a prominent problem for advanced cancer patients and is associated with both decreased quality of life and poor prognosis. More than one million cancer patients in the United States are affected by cachexia.[57] Patients with cachexia and their families pay a tremendous price physically, emotionally, and financially, attempting to cope with this condition. The financial burden of health care, including length and cost of hospitalization, is growing steadily, and all patients with cachexia face this added hardship.[58] However,

a consistently efficacious and approved therapeutic option for cachexia is currently lacking, making earlier diagnosis and assessment of cachexia risk all the more critical in cancer patients. Our study posits activated skeletal muscle-resident mast cells as a tool for assessing cancer patient risk for cachexia development, in order to improve cachexia diagnoses as well as patient quality of life and prognoses.

Author contributions

D.B.W. and Y.S. wrote the manuscript with input from all authors. All authors reviewed and approved the final manuscript. D.B.W., S.H.P., M.R.E., C. L., D.C.F., and Y.S. designed study and contributed to data interpretation. D.B.W. and C. L. performed animal studies. D.B.W. and S.S. performed immunohistochemistry and quantification analyses. Q.Z. performed western blot and quantification analyses. D.C.F. and Y.S. supervised the study.

Acknowledgements

We would like to thank Drs Osvaldo Delbono and Tracy Criswell (Wake Forest University Health Sciences) for the constructive discussion and technical support. This work is directly supported by the National Cancer Institute (R01-CA238888, Y.S.; R44-CA203184, Y.S.), Department of Defence (W81XWH-17-1-0541, Y.S.; W81XWH-19-1-0045, Y.S.), METAvivor (METAvivor Research Award, Y.S.), and the Wake Forest Baptist Comprehensive Cancer Center Internal Pilot Funding (Y.S.). This work is also supported by the National Cancer Institute's Cancer Center Support Grant award number P30-CA012197 issued to the Wake Forest Baptist Comprehensive Cancer Center. The authors wish to acknowledge the support of the Wake Forest Baptist Comprehensive Cancer Center Cell Engineering Shared Resource and Flow Cytometry Shared Resource, supported by the National Cancer Institute's Cancer Center Support Grant award number P30-CA012197. The content is solely the responsibility of the authors and does not necessarily represent the official views of the National Cancer Institute and Department of Defense. The authors of this manuscript certify that they comply with the ethical guidelines for authorship and publishing in the Journal of Cachexia, Sarcopenia and Muscle.[59]

Conflict of interests

Yusuke Shiozawa has received research funding from TEVA Pharmaceuticals, but not relevant to this study. No conflict of interest exists for remaining authors.

References

1. Onesti JK, Guttridge DC. Inflammation based regulation of cancer cachexia. *Biomed Res Int* 2014;**2014**:168407.
2. Fearon K, Strasser F, Anker SD, Bosaeus I, Bruera E, Fainsinger RL, et al. Definition and classification of cancer cachexia: an international consensus. *Lancet Oncol* 2011;**12**:489–495.
3. Al-Majid S, Waters H. The biological mechanisms of cancer-related skeletal muscle wasting: the role of progressive resistance exercise. *Biol Res Nurs* 2008;**10**:7–20.
4. Porporato PE. Understanding cachexia as a cancer metabolism syndrome. *Oncogenesis* 2016;**5**:e200.
5. Penet MF, Bhujwalla ZM. Cancer cachexia, recent advances, and future directions. *Cancer J* 2015;**21**:117–122.
6. Mueller TC, Bachmann J, Prokopchuk O, Friess H, Martignoni ME. Molecular pathways leading to loss of skeletal muscle mass in cancer cachexia—can findings from animal models be translated to humans? *BMC Cancer* 2016;**16**:75.
7. Ni J, Zhang L. Cancer cachexia: definition, staging, and emerging treatments. *Cancer Manag Res* 2020;**12**:5597–5605.
8. Narsale AA, Carson JA. Role of interleukin-6 in cachexia: therapeutic implications. *Curr Opin Support Palliat Care* 2014;**8**:321–327.
9. Weiss K, Mu X, Agarwal R. *Notch signaling and inflammation in a murine model of sarcoma-associated cachexia [abstract]*. Philadelphia, PA: AACR Cancer Research; 2015.
10. Acharyya S, Ladner KJ, Nelsen LL, Damrauer J, Reiser PJ, Swoap S, et al. Cancer cachexia is regulated by selective targeting of skeletal muscle gene products. *J Clin Invest* 2004;**114**:370–378.
11. Jatoi A, Dakhil SR, Nguyen PL, Sloan JA, Kugler JW, Rowland KM, et al. A placebo-controlled double blind trial of etanercept for the cancer anorexia/weight loss syndrome: results from N00C1 from the North Central Cancer Treatment Group. *Cancer* 2007;**110**:1396–1403.
12. Wu C, Fernandez SA, Criswell T, Chidiac TA, Guttridge D, Villalona-Calero M, et al. Disrupting cytokine signaling in pancreatic cancer: a phase I/II study of etanercept in combination with gemcitabine in patients with advanced disease. *Pancreas* 2013;**42**:813–818.
13. Wernersson S, Pejler G. Mast cell secretory granules: armed for battle. *Nat Rev Immunol* 2014;**14**:478–494.
14. Urb M, Sheppard DC. The role of mast cells in the defence against pathogens. *PLoS Pathog* 2012;**8**:e1002619.
15. Yokota M, Suzuki K, Tokoyoda K, Meguro K, Hosokawa J, Tanaka S, et al. Roles of mast cells in the pathogenesis of inflammatory myopathy. *Arthritis Res Ther* 2014;**16**:R72.
16. Radley HG, Grounds MD. Cromolyn administration (to block mast cell degranulation) reduces necrosis of dystrophic muscle in mdx mice. *Neurobiol Dis* 2006;**23**:387–397.
17. Bonetto A, Aydogdu T, Kunzevitzky N, Guttridge DC, Khuri S, Koniaris LG, et al. STAT3 activation in skeletal muscle links muscle wasting and the acute phase response in cancer cachexia. *PLoS One* 2011;**6**:e22538.
18. Edgar R, Domrachev M, Lash AE. Gene expression omnibus: NCBI gene expression and hybridization array data repository. *Nucleic Acids Res* 2002;**30**:207–210.
19. Barrett T, Wilhite SE, Ledoux P, Evangelista C, Kim IF, Tomashevsky M, et al. NCBI GEO: archive for functional genomics data sets—

update. *Nucleic Acids Res* 2013;**41**: D991–D995.
20. Gallagher IJ, Stephens NA, MacDonald AJ, Skipworth RJ, Husi H, Greig CA, et al. Suppression of skeletal muscle turnover in cancer cachexia: evidence from the transcriptome in sequential human muscle biopsies. *Clin Cancer Res* 2012;**18**: 2817–2827.
21. Callaway CS, Delitto AE, Patel R, Nosacka RL, D'Lugos AC, Delitto D, et al. IL-8 released from human pancreatic cancer and tumor-associated stromal cells signals through a CXCR2-ERK1/2 axis to induce muscle atrophy. *Cancers (Basel)* 2019;**11**:1863.
22. The Gene Ontology C. The gene ontology resource: 20 years and still GOing strong. *Nucleic Acids Res* 2019;**47**:D330-D8.
23. Ashburner M, Ball CA, Blake JA, Botstein D, Butler H, Cherry JM, et al. Gene ontology: tool for the unification of biology. *The Gene Ontology Consortium Nat Genet* 2000;**25**:25–29.
24. Subramanian A, Tamayo P, Mootha VK, Mukherjee S, Ebert BL, Gillette MA, et al. Gene set enrichment analysis: a knowledge-based approach for interpreting genome-wide expression profiles. *Proc Natl Acad Sci U S A* 2005;**102**:15545–15550.
25. Liberzon A, Subramanian A, Pinchback R, Thorvaldsdottir H, Tamayo P, Mesirov JP. Molecular signatures database (MSigDB) 3.0. *Bioinformatics* 2011;**27**:1739–1740.
26. Liberzon A. A description of the Molecular Signatures Database (MSigDB) Web site. *Methods Mol Biol* 2014;**1150**: 153–160.
27. Mootha VK, Lindgren CM, Eriksson KF, Subramanian A, Sihag S, Lehar J, et al. PGC-1alpha-responsive genes involved in oxidative phosphorylation are coordinately downregulated in human diabetes. *Nat Genet* 2003;**34**:267–273.
28. Consortium GT. The genotype-tissue expression (GTEx) project. *Nat Genet* 2013;**45**:580–585.
29. Tang Z, Kang B, Li C, Chen T, Zhang Z. GEPIA2: an enhanced web server for large-scale expression profiling and interactive analysis. *Nucleic Acids Res* 2019;**47**: W556–W560.
30. Judge SM, Nosacka RL, Delitto D, Gerber MH, Cameron ME, Trevino JG, et al. Skeletal muscle fibrosis in pancreatic cancer patients with respect to survival. *JNCI Cancer Spectr* 2018;**2**:pky043.
31. Files DC, D'Alessio FR, Johnston LF, Kesari P, Aggarwal NR, Garibaldi BT, et al. A critical role for muscle ring finger-1 in acute lung injury-associated skeletal muscle wasting. *Am J Respir Crit Care Med* 2012;**185**:825–834.
32. Shi SR, Chaiwun B, Young L, Cote RJ, Taylor CR. Antigen retrieval technique utilizing citrate buffer or urea solution for immunohistochemical demonstration of androgen receptor in formalin-fixed paraffin sections. *J Histochem Cytochem* 1993;**41**: 1599–1604.
33. Cruse G, Gilfillan AM, Smrz D. Flow cytometry-based monitoring of mast cell activation. *Methods Mol Biol* 2015;**1220**: 365–379.
34. Meurer SK, Neß M, Weiskirchen S, Kim P, Tag CG, Kauffmann M, et al. Isolation of mature (peritoneum-derived) mast cells and immature (bone marrow-derived) mast cell precursors from mice. *PLoS One* 2016;**11**:e0158104.
35. Menconi M, Gonnella P, Petkova V, Lecker S, Hasselgren PO. Dexamethasone and corticosterone induce similar, but not identical, muscle wasting responses in cultured L6 and C2C12 myotubes. *J Cell Biochem* 2008;**105**:353–364.
36. Kohler S, Gargano M, Matentzoglu N, Carmody LC, Lewis-Smith D, Vasilevsky NA, et al. The human phenotype ontology in 2021. *Nucleic Acids Res* 2021;**49**: D1207–D1217.
37. Payne V, Kam PC. Mast cell tryptase: a review of its physiology and clinical significance. *Anaesthesia* 2004;**59**:695–703.
38. Pelekanou V, Villarroel-Espindola F, Schalper KA, Pusztai L, Rimm DL. CD68, CD163, and matrix metalloproteinase 9 (MMP-9) co-localization in breast tumor microenvironment predicts survival differently in ER-positive and -negative cancers. *Breast Cancer Res* 2018;**20**:154.
39. Deboer MD. Animal models of anorexia and cachexia. *Expert Opin Drug Discovery* 2009;**4**:1145–1155.
40. Choi E, Carruthers K, Zhang L, Thomas N, Battaglino RA, Morse LR, et al. Concurrent muscle and bone deterioration in a murine model of cancer cachexia. *Physiol Rep* 2013;**1**:e00144.
41. Iwata Y, Suzuki N, Ohtake H, Kamauchi S, Hashimoto N, Kiyono T, et al. Cancer cachexia causes skeletal muscle damage via transient receptor potential vanilloid 2-independent mechanisms, unlike muscular dystrophy. *J Cachexia Sarcopenia Muscle* 2016;**7**:366–376.
42. Aulino P, Berardi E, Cardillo VM, Rizzuto E, Perniconi B, Ramina C, et al. Molecular, cellular and physiological characterization of the cancer cachexia-inducing C26 colon carcinoma in mouse. *BMC Cancer* 2010;**10**:363.
43. Wang Y, Pessin JE. Mechanisms for fiber-type specificity of skeletal muscle atrophy. *Curr Opin Clin Nutr Metab Care* 2013;**16**:243–250.
44. Yuan L, Han J, Meng Q, Xi Q, Zhuang Q, Jiang Y, et al. Muscle-specific E3 ubiquitin ligases are involved in muscle atrophy of cancer cachexia: an in vitro and in vivo study. *Oncol Rep* 2015;**33**: 2261–2268.
45. Li YP, Reid MB. NF-kappaB mediates the protein loss induced by TNF-alpha in differentiated skeletal muscle myotubes. *Am J Physiol Regul Integr Comp Physiol* 2000;**279**:R1165–R1170.
46. Moon TC, Befus AD, Kulka M. Mast cell mediators: their differential release and the secretory pathways involved. *Front Immunol* 2014;**5**:569.
47. Beck SC, Wilding T, Buka RJ, Baretto RL, Huissoon AP, Krishna MT. Biomarkers in human anaphylaxis: a critical appraisal of current evidence and perspectives. *Front Immunol* 2019;**10**:494.
48. Banduseela V, Ochala J, Lamberg K, Kalimo H, Larsson L. Muscle paralysis and myosin loss in a patient with cancer cachexia. *Acta Myol* 2007;**26**:136–144.
49. Cosper PF, Leinwand LA. Myosin heavy chain is not selectively decreased in murine cancer cachexia. *Int J Cancer* 2012;**130**: 2722–2727.
50. Yamada T, Ashida Y, Tatebayashi D, Abe M, Himori K. Cancer cachexia induces preferential skeletal muscle myosin loss when combined with denervation. *Front Physiol* 2020;**11**:445.
51. Trias E, King PH, Si Y, Kwon Y, Varela V, Ibarburu S, et al. Mast cells and neutrophils mediate peripheral motor pathway degeneration in ALS. *JCI Insight* 2018;**3**.
52. Costa RGF, Caro PL, de Matos-Neto EM, Lima J, Radloff K, Alves MJ, et al. Cancer cachexia induces morphological and inflammatory changes in the intestinal mucosa. *J Cachexia Sarcopenia Muscle* 2019;**10**: 1116–1127.
53. Shukla SK, Markov SD, Attri KS, Vernucci E, King RJ, Dasgupta A, et al. Macrophages potentiate STAT3 signaling in skeletal muscles and regulate pancreatic cancer cachexia. *Cancer Lett* 2020;**484**:29–39.
54. Cregar L, Elrod KC, Putnam D, Moore WR. Neutrophil myeloperoxidase is a potent and selective inhibitor of mast cell tryptase. *Arch Biochem Biophys* 1999;**366**: 125–130.
55. Molderings GJ, Brettner S, Homann J, Afrin LB. Mast cell activation disease: a concise practical guide for diagnostic workup and therapeutic options. *J Hematol Oncol* 2011;**4**:10.
56. Akin C, Valent P, Metcalfe DD. Mast cell activation syndrome: proposed diagnostic criteria. *J Allergy Clin Immunol* 2010;**126**: 1099–1104 e4.
57. Morley JE, Thomas DR, Wilson MM. Cachexia: pathophysiology and clinical relevance. *Am J Clin Nutr* 2006;**83**:735–743.
58. Arthur ST, Noone JM, Van Doren BA, Roy D, Blanchette CM. One-year prevalence, comorbidities and cost of cachexia-related inpatient admissions in the USA. *Drugs Context* 2014;**3**:212265.
59. von Haehling S, Morley JE, Coats AJS, Anker SD. Ethical guidelines for publishing in the Journal of Cachexia, Sarcopenia and Muscle: update 2019. *J Cachexia Sarcopenia Muscle* 2019;**10**:1143–1145.